**SUPPLEMENT**

**Enrichr analyses of panels of clustered upregulated genes from iLINCS clustering analysis**

We began by using Enrichr to identify pathways associated with our panels of clustered upregulated genes from our iLINCS clustering analysis (Figure 3, Figures S4-S10). Using KEGG, we generated top cell signaling pathways which returned hits such as FOXO, Wnt, and MAPK signaling. FOXO1 is localized to the nucleus where it binds to the insulin response sequence located in the promoter for glucose 6-phosphatase and increases its rate of transcription (71). The FOXO transcription factor family is regulated by an array of posttranslational modifications, including phosphorylation (60). FOXO has also been implicated in diabetes complications, and transgenic mice that overexpress FOXO1 have impaired glucose tolerance and a suppression of genes involved in glucose utilization by glycolysis, the pentose phosphate shunt, and lipogenesis (72).

Wnt signaling pathways play a role in inflammation and metabolic regulation, including shifts in fuel utilization between glycolysis and fatty acid oxidation (62, 73). Abnormal Wnt signaling is linked to altered expression of key metabolic genes, transcription factors, and proteins associated with mitochondrial dysfunction and carbohydrate metabolism (73-76). Wnt pathways can modulate T-cell factor (TCF) transcriptional activity, and in turn target genes such as MYC and PPARδ, which are linked to mitochondrial glutaminolysis and oxidative capacity (77, 78).

MAPKs have the ability to respond to and regulate key metabolic targets, and are activated in response to insulin. However, inappropriate MAPK signaling can result in metabolic syndrome (61). When phosphorylated, MAPKs such as ERK1/2 and p38 have the ability to enhance the transcriptional activity of peroxisome proliferator-activated receptors (PPARs), and in turn alter glucose uptake (79). Alternatively, prolonged inhibition of the p38 alters the expression levels of glucose transporters GLUT1/GLUT4 and decreases glucose uptake (80).

The top hits in our GO molecular function analysis for panels of clustered upregulated genes included the PKC family of enzymes, which typically catalyze phosphorylation reactions and transduce signals that promote lipid hydrolysis, regulated cell growth, and mediate the inflammatory response (81). PKCs also have the ability to activate MAPKs, altering the gene expression, the cellular phenotype, and induce diabetic complications (82). Taken together, top signaling pathways for our panels of clustered upregulated genes implicate glucose utilization, energy homeostasis, mitochondrial function, and cell growth.

The top hit of our protein-protein interaction analysis for panels of clustered upregulated genes was RPS6KA3, a gene that encodes a member of the ribosomal S6 kinase (RSK) family of growth factor-regulated serine/threonine kinases. These kinases phosphorylate many targets, and are key in in cell cycle progression, differentiation, and cell survival (83). The second hit in our analysis was MAPK14. RSK proteins appear to have important roles in cell cycle progression, differentiation, and cell survival, and are directly phosphorylated and activated by MAPK proteins (such as ERK1) (83). In primary neurons, n-methyl-D-aspartate receptor (NMDAR) activation leads to ERK and RSK2 activation. (84). Recent evidence suggests that RSK2 regulates AMPA receptor transmission, and could be important for neuroplastic events such as learning and memory (84). Other kinase hits include glycogen synthase kinase 3 beta (GSK3B) and cyclin dependent kinase 1 (CDK1), which are heavily involved in energy metabolism, mitochondrial respiration, and cell-cycle progression (85, 86). We also found hits for two core subunits of the SKP1-CUL1-F-box protein E3 ubiquitin ligase complex, CUL1 and SKP1, that regulate ubiquitination of cell proliferation proteins (87). Taken together, our top protein-protein interaction hits suggest a role for pathways involved in energy metabolism and cell proliferation.

Next, we probed for kinases that when knocked down in specific cell lines, increased the expression of genes that were in our panels of clustered upregulated genes. We found several serine/threonine-protein kinases including AKT1, PTK2, MAP2K2, and ATR. AKT1 is one of 3

closely related serine/threonine-protein kinases (AKT1, AKT2 and AKT3) thought to regulate metabolism and promote cellular proliferation (88). AKT also phosphorylates GSK-3 (stimulating glycogen synthesis) and modulates glucose uptake via increased GLUT1 transcription and targeting of GLUT4 to the plasma membrane (89). Interestingly, genetic linkage studies have identified AKT as a candidate susceptibility gene for schizophrenia, and AKT1 protein expression and kinase activity are decreased in schizophrenia (90-92). Protein-tyrosine kinase 2 (PTK2) plays an important role in cellular adhesion, migration, and cytoskeletal functions (93). Mitogen-activated protein kinase kinase 2 (MAP2K2) codes for the protein MEK2, which is part of the RAS/MAPK signaling, and regulates cell proliferation, differentiation, migration, and apoptosis (94). Similarly, ATR regulates the cell cycle by activating checkpoint damage signaling (95).

We also had significant hits for G-protein coupled receptor proteins NMUR2 and FFAR1. Neuromedin U (NMUR2) encodes a G-protein coupled receptor protein widely expressed in the central nervous system (CNS) that binds the neuropeptide neuromedin U in order to regulate energy homeostasis (96, 97). Free fatty acid receptor 1 (FFAR1) is another membrane protein in the G-protein coupled receptor family that binds medium to long chain free fatty acids, is widely expressed in the brain, and helps in the regulation of energy homeostasis (98). FFAR1 is transcriptionally upregulated by glucose, which is blocked via PI3K inhibitors such as Wortmannin, suggesting a PI3K dependent mechanism (99). Interestingly, FFAR1 agonists are considered potential drug interventions to enhance insulin secretion in type 2 diabetes (99). Taken together, these results suggest that kinases involved in glucose metabolism and cell cycle regulation are relevant to our panels of clustered upregulated genes.

Finally, we performed pathway analyses to identify transcription factors with occupancy sites for our panels of clustered upregulated genes, several of which played key roles in neurodevelopment. For example, WT1 is a tumor suppressor gene that plays an important role in cellular development and is essential in the development of the urogenital system (100), while

NFIB is essential in tissue differentiation in embryonic development (101). Similarly, TCF3 regulates many developmental processes such as CNS development (102). For instance, TCF3 represses Wnt–β-Catenin signaling during neocortical development (103). Lastly, TRIM28 is a ubiquitously expressed protein involved in transcriptional regulation, cellular differentiation and proliferation, and apoptosis (104). Interestingly, deletion of this protein in adult mice results in increased anxiety-like behaviors and stress-induced alterations in stress-induced alterations in spatial learning and memory (105). Our transcription factor analysis also generated hits for estrogen receptors (ESR1, ESR2), tumor suppressors/activators (ELK3), and transcription factors involved in immune responses and macrophage function (CEBPB)(106, 107).

**Enrichr analyses of panels of clustered downregulated genes from iLINCS clustering analysis**

We began by using Enrichr to identify pathways associated with our panels of clustered downregulated genes from our iLINCS clustering analysis (Figure 4, Figures S11-S17). Using KEGG, we generated top cell signaling pathways which returned hits such as HTLV infection, hepatitis B, p53 signaling, and cell cycle pathways. This implicates inflammation, impaired immunity, and cell proliferation. For instance, p53 is a highly studied tumor suppressor that regulates the expression of >2,500 target genes impacting cellular processes such as cell longevity, while hepatitis B causes acute and chronic necroinflammatory liver diseases involving the adaptive immune response (108, 109).

The top 5 hits in our GO cellular components analysis for panels of clustered downregulated genes implicate the mitochondria and oxidative phosphorylation (Figure S12). Implicated cellular components included include 2 cardiac mitochondria (subsarcolemmal and interfibrillar mitochondria), two spermatid mitochondria (Nebenkern and mitochondrial derivative), and general mitochondrion, possibly indicating widespread bioenergetic abnormalities.

The top hit of our protein-protein interaction analysis (Figure S14) for panels of clustered

downregulated genes was histone deacetylase 2 (HDAC2), a ubiquitously expressed protein that removes acetyl groups from lysine residues on core histones (110). When histones are modified by deacetylation (or other posttranslational modifications), chromatin properties and thus DNA packaging and many central biological processes can be affected (111). HDAC1, another histone deacetylase, and its binding partners proliferating cell nuclear antigen (PCNA) and BRCA1 are involved in epigenetics and DNA replication, and DNA repair (112). Epigenetic repression via histone deacetylation could play a key role in development, transcriptional regulation, and cell cycle progression (111). For instance, an HDAC1 complex deacetylates p53, one of our significantly implicated cell pathways, which in turn can modulate p53-mediated cell growth arrest and apoptosis (113). Interestingly, HDAC1 is increased in the prefrontal cortex and hippocampus in schizophrenia and overexpression of HDAC1 leads to impairments in working memory (114-116). Similarly, neuron-specific overexpression of HDAC2 in mice led to suppression of spine formation, reduced synapse number, and impaired synaptic plasticity and memory formation, changes observed in chronic schizophrenia (117). These morphological changes and learning impairments were ameliorated by treatment with the HDAC inhibitor suberoylanilide hydroxamic acid (SAHA; vorinostat), suggesting a possible therapeutic role for HDAC inhibitors in the treatment of schizophrenia (117). Supporting this hypothesis, there are accumulating instances of schizophrenia patients with mutations in genes encoding chromatin regulators (such as histone modifying enzymes and transcription factors) (118). On a broader scale, meta-analyses from genome-wide association studies (GWAS) and postmortem transcriptomic data implicate chromatin and nucleosome assembly machinery may contribute to the genetic risk of schizophrenia (119, 120).

Another one of our top hits was CREB-binding protein (CREBBP), a ubiquitously expressed protein with intrinsic histone acetyltransferase activity (121). It is involved in the transcriptional coactivation of several transcription factors, playing crucial roles in development, promoting cell growth, and energy homeostasis (122). For example, CREBBP acetylates p53,

E2F, and TCF4 transcription factors affecting their transcriptional activation and DNA binding activities (123-125). Additionally, normal levels of CREBBP are essential for repressing MYC, another top protein-protein interactor, in the G1 phase of the cell cycle, thereby preventing inappropriate entry of cells into S phase (126). MYC is normally activated by Wnt and EGF (via the MAPK/ERK pathway), and universally upregulates gene expression to promote cell cycle progression (127-129). Taken together, these results indicate a disruption in the balance of activation and suppression of cellular proliferation processes.

Another hit in our protein-protein interaction analysis was casein kinase 2 alpha 1 (CSNK2A1), a catalytic subunit of casein kinase 2 (CK2), the constitutively active serine/threonine-protein kinase. CK2 promotes cell survival in part by phosphorylating AKT and stimulating the Wnt signaling pathway (130, 131), systems that were implicated in our KEGG and kinase analysis of panels of clustered upregulated genes. CK2 is constituently active and also has a regulatory role in p53/MAPK signaling, further implicating cellular processes such as cell cycle progression, proliferation, and suppression of apoptosis (132-134).

Lastly, we had a hit for NFKB2, a transcription factors with essential roles in innate immunity and inflammation (135, 136). Mutations in the NFKB2 gene or protein can result in immunodeficiency syndromes (137, 138). The NFKB family is known for directly binding several transcription factors including p53 (139). Stimulation of NFKB promotes resistance to p53 mediated apoptosis, as p53 and NFKB inhibit each other's ability to stimulate gene expression (140). There is also evidence that NFKB interacts with numerous upstream kinases, chromatin-modifiers such as HDACs, and CREBBP (141-143).

Next, we probed for kinases that when knocked down in specific cell lines, decreased the expression of genes that were in our panels of clustered downregulated genes (Figure S15). We found multiple kinases with important roles in glucose homeostasis and energy metabolism. The nuclear receptor PPARγ forms a heterodimer with the retinoid X receptor (RXR), two of our top hits, increasing the transcription of various genes that stimulate glucose uptake and

carbohydrate metabolism (144). PPARγ ligands such as thiazolidinediones (TZDs), increase glucose utilization, treat hyperglycemia, and represent therapeutic possibilities in disease signatures with deficient glycolytic systems (145). PPARγ also regulates gut homeostasis by potently inhibiting inflammatory mediator-induced NFKB transcriptional activity (146). For other PPAR family members such as PPARα, RXRA heterodimerization is required for transcriptional activation on fatty oxidation genes (144). PXK, another hit, also is highly involved in energy metabolism via modulation of $Na^+/K^+$-ATPase enzymatic and ion pump activities (147). Recent work also demonstrated our hit ABL2, a cytoplasmic tyrosine kinase, is activated in the cellular response to oxidative stress (148).

We also found kinases that are involved in axonal growth during CNS development (RYK), cell growth and cycle progression (WEE1, ABL2), and cytoskeletal remodeling (ABL2). RYK is a Wnt receptor important in neurogenesis and axon guidance that also interacts with significant transcription factors from our analyses such as FOXO (149, 150). ABL2, although involved in oxidative stress, also has significant cytoskeletal remodeling functions (151). Similarly, top hit LPHN1 functions in cell adhesion and growth (152). WEE1 is a nuclear kinase important in the regulation of cell size, which it accomplishes via inhibition of CDK1, effectively governing the time point of mitosis entry (153). We also report NR3C1 and GPR37 as significant kinases. NR3C1 is a glucocorticoid receptor regulating genes involved in development, metabolism, and immune responses (154). NR3C1 has the ability to bind to and transrepress other transcription factors such as NFKB, and thus exert anti-inflammatory actions (155). Taken together, these results suggest that kinases involved in carbohydrate/fatty acid metabolism, inflammation, and cell cycle regulation are relevant to our panels of clustered downregulated genes.

Finally, we performed pathway analyses to identify transcription factors with occupancy sites for our panels of clustered downregulated genes, several of which played key roles in cellular proliferation/development and were similar to hits from previous analyses (MYC, MYCN,

NUCKS1, forkhead box M1) (Figure S16). We also report additional transcription factors that play crucial roles in cell cycle control such as tumor suppressor proteins E2F1 and E2F4 (156). These transcription factors suggest a connection between our disease signature and regulatory elements of the cell cycle throughout the course of development.

In summary, we extrapolated on the abnormalities of glycolytic enzymes using Enrichr pathway analyses. These analyses yield additional pathways and regulators involved in cellular processes such as cell cycle regulation and inflammatory responses. Inappropriate cell cycle regulation could contribute to metabolic deficits, while the immune system has previously been implicated in schizophrenia (157-159). Several of our metabolic and immunity findings were replicated in other large scale transcriptomic bioinformatic analyses of psychiatric disorders (160). These results highlight the connectivity of glycolytic pathology in schizophrenia to several systems that could be important targets in future studies (Table 3).

**SUPPLEMENTARY FIGURES**

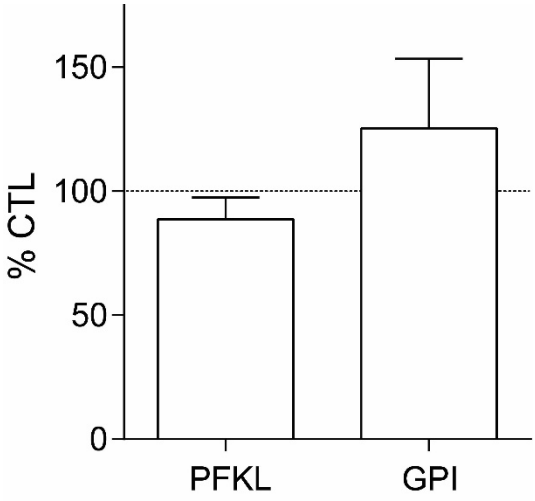


**Figure S1. mRNA expression in astrocytes.** Relative expression levels of glucose-6-phosphate isomerase (GPI) and phosphofructokinase liver (PFKL) transcripts in enriched astrocytes populations from schizophrenia (SCZ, n=16) and control (CTL, n=16) subjects (A). Data from astrocyte enriched samples were normalized to the geometric mean of three housekeeping genes. Data are expressed as percent control ± SEM. *P<0.05.

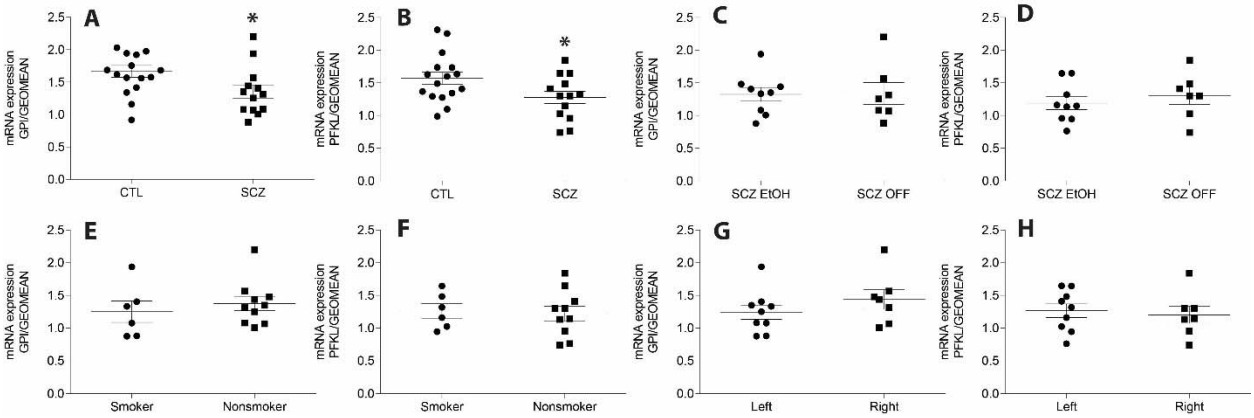


**Figure S2. Secondary analysis postmortem LCM-qPCR findings.** Antipsychotic naïve patients were excluded from cell-level analysis and targets remained significant (GPI p=0.034, PFKL p=0.037) (A, B). We performed secondary analyses of schizophrenia subjects on and off EtOH (C, D), smokers/nonsmokers (E, F), and samples from the left or right brain (G, H) and did not detect an effect. Control (CTL), glucose phosphate isomerase (GPI), phosphofructokinase liver type (PFKL). Data were normalized to the geometric mean of three housekeeping genes and expressed ± SEM. *P<0.05.

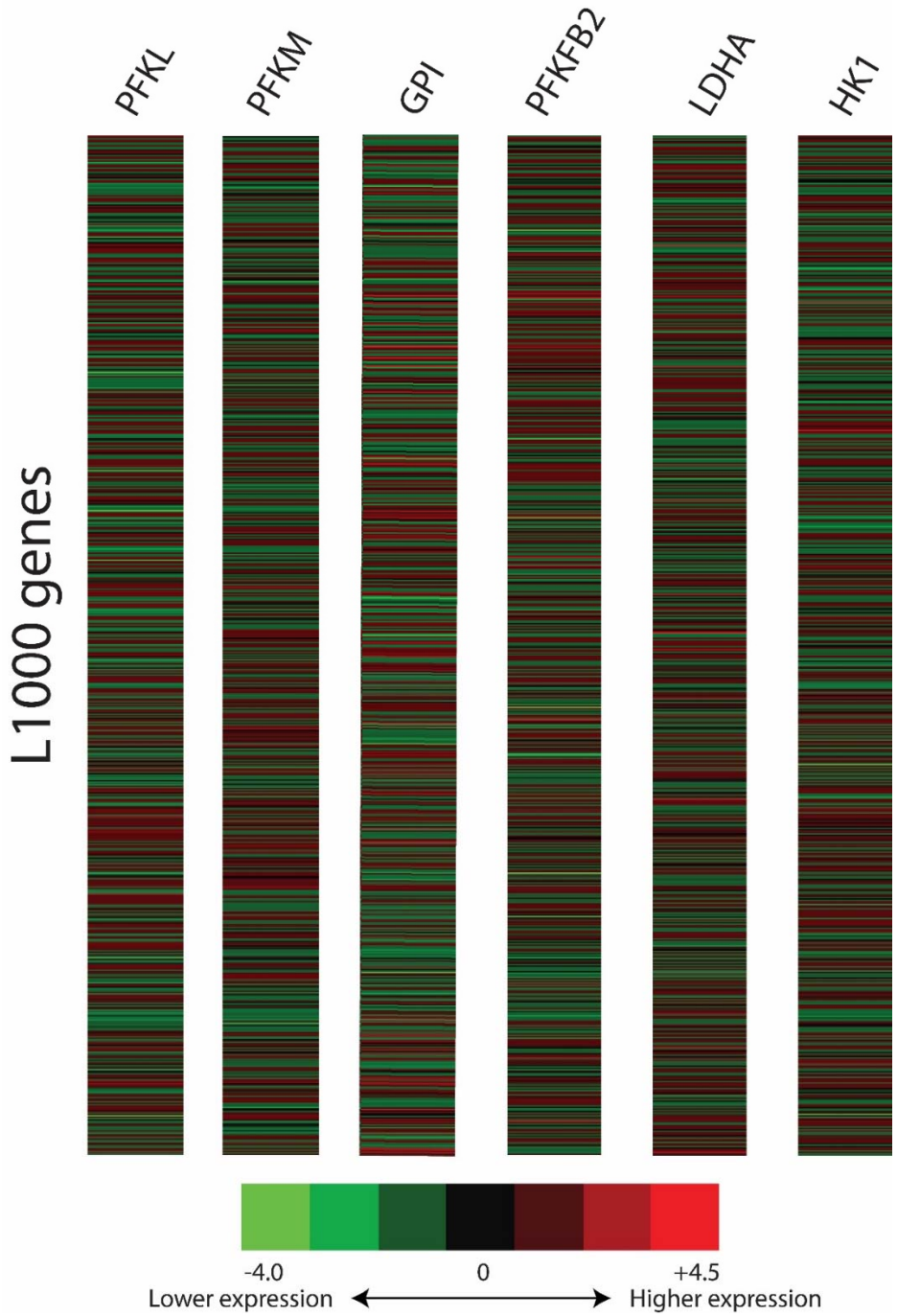


**Figure S3. Heatmap of seed gene knockdown signatures.** Representative heatmaps of transcriptional changes in all L1000 genes in each seed gene knockdown signature. The L1000 genes are arranged in alphabetical order on the y-axis and is consistent across signatures in this figure (each row represents expression of the same L1000 gene across the KD signatures). Phosphofructokinase liver type (PFKL); PFK muscle type (PFKM); G lucose-6-phosphate

isomerase (GPI); 6-phosphofructo-2-kinase (PFKFB2); lactate dehydrogenase A (LDHA); hexokinase 1 (HK1).


**Figure S4. Enrichr analyses: KEGG cell signaling pathways for panels of clustered upregulated genes.**

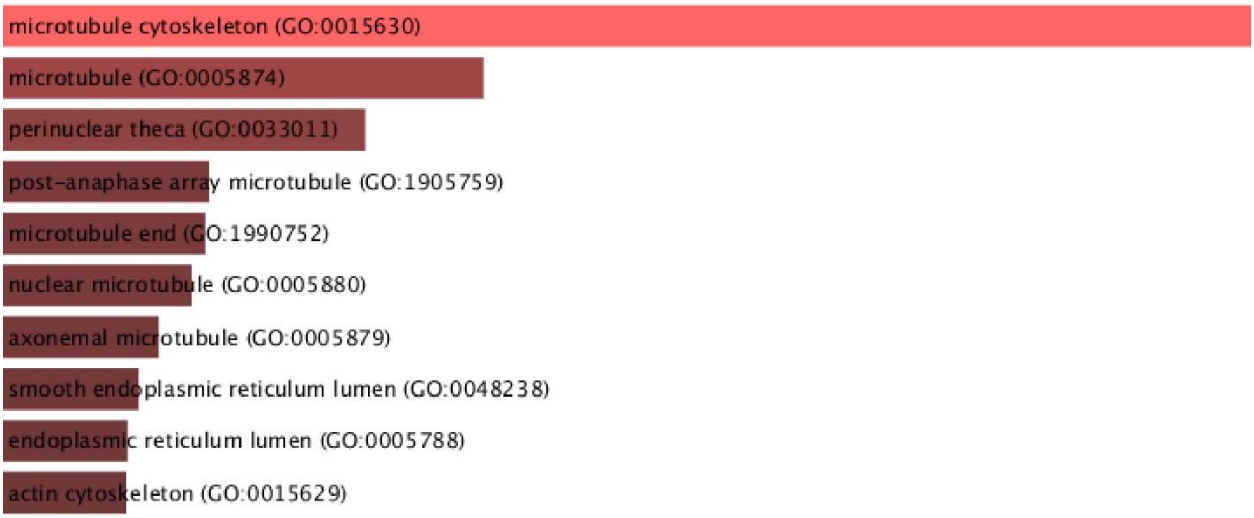


**Figure S5. Enrichr analyses: Cellular components for panels of clustered upregulated genes.**

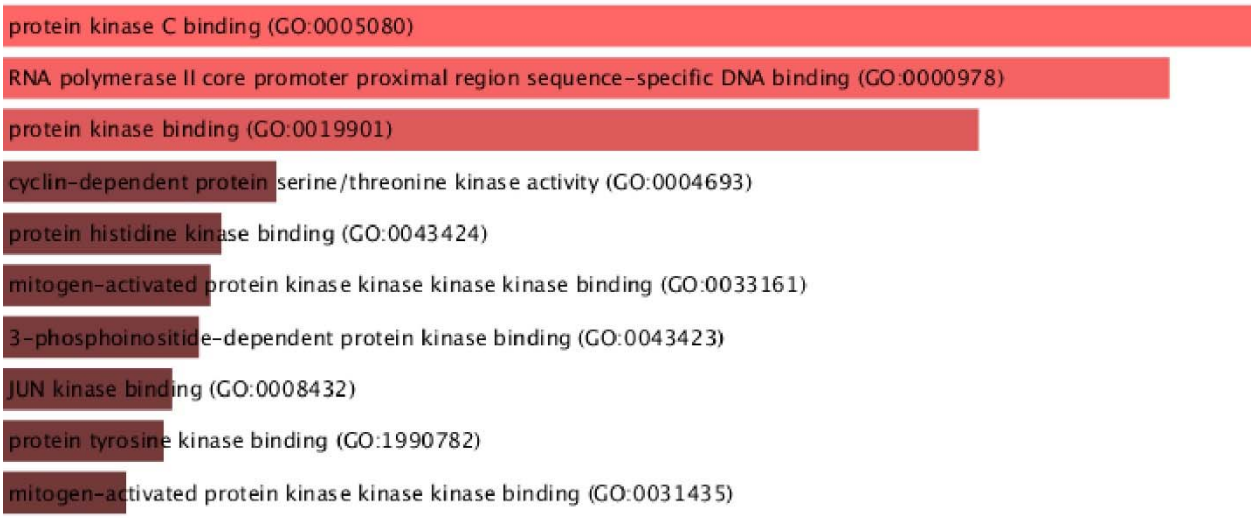


**Figure S6. Enrichr analyses: Molecular function for panels of clustered upregulated genes.**

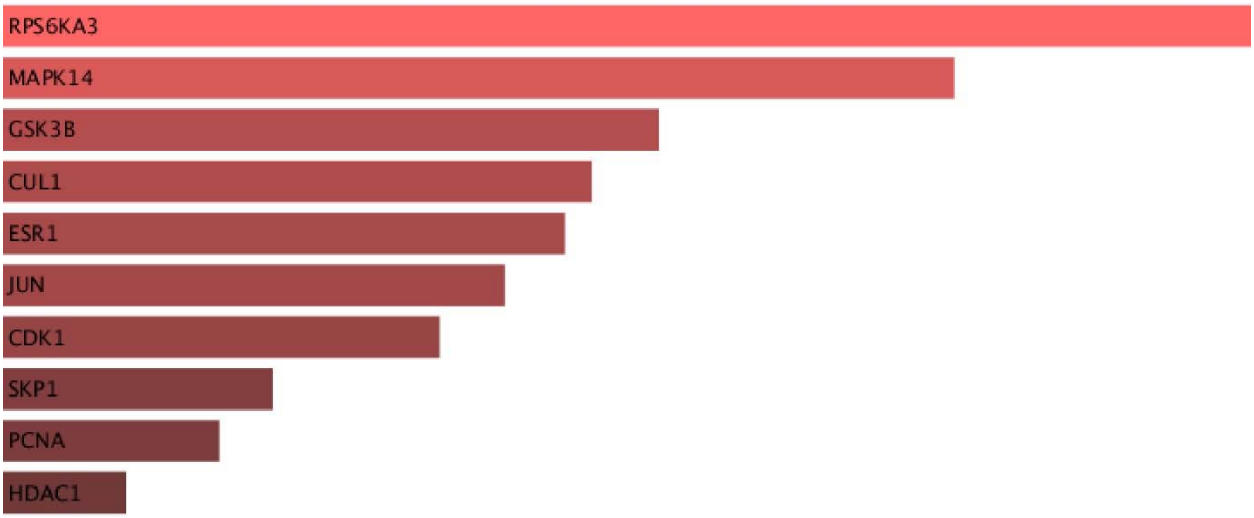


**Figure S7. Enrichr analyses: Protein-protein interaction hubs for panels of clustered upregulated genes.**

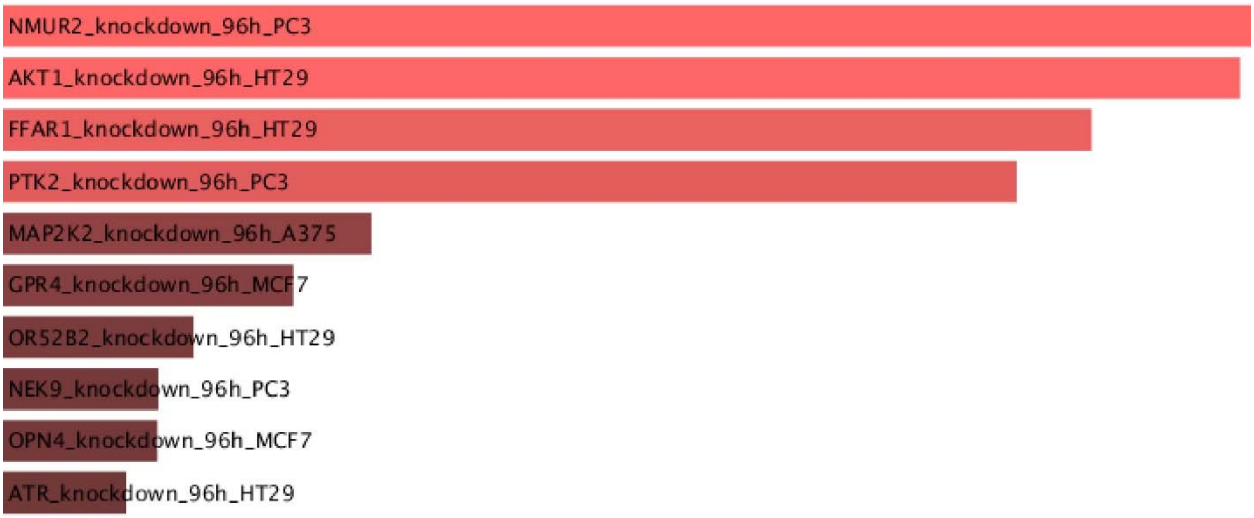


**Figure S8. Enrichr analyses: Kinase analysis for panels of clustered upregulated genes.**

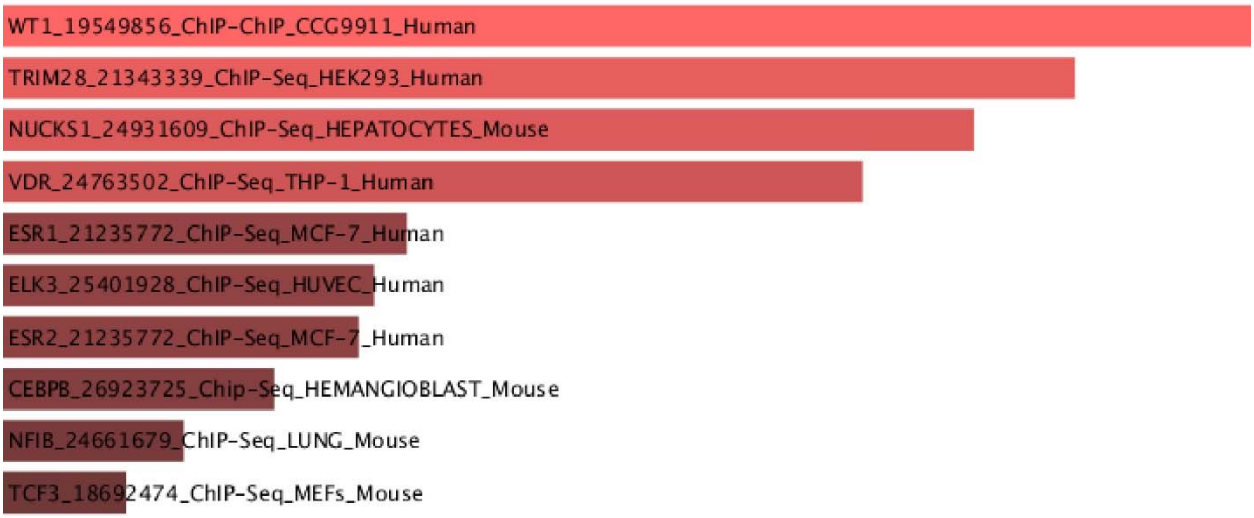


**Figure S9. Enrichr analyses: Transcription factor analysis for panels of clustered upregulated genes.**

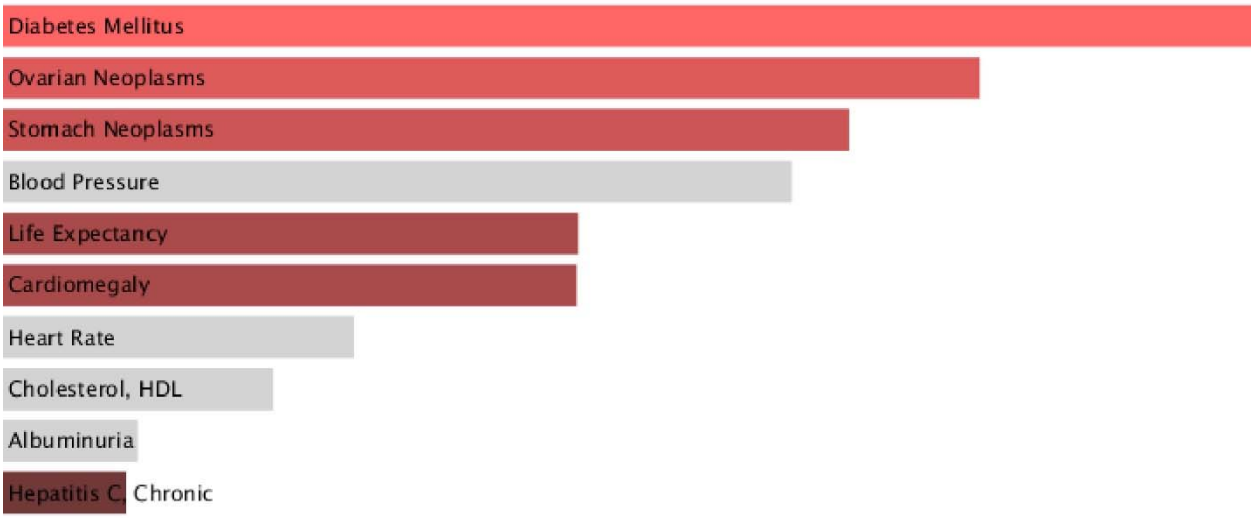


**Figure S10. Enrichr analyses: dbGaP for panels of clustered upregulated genes.**

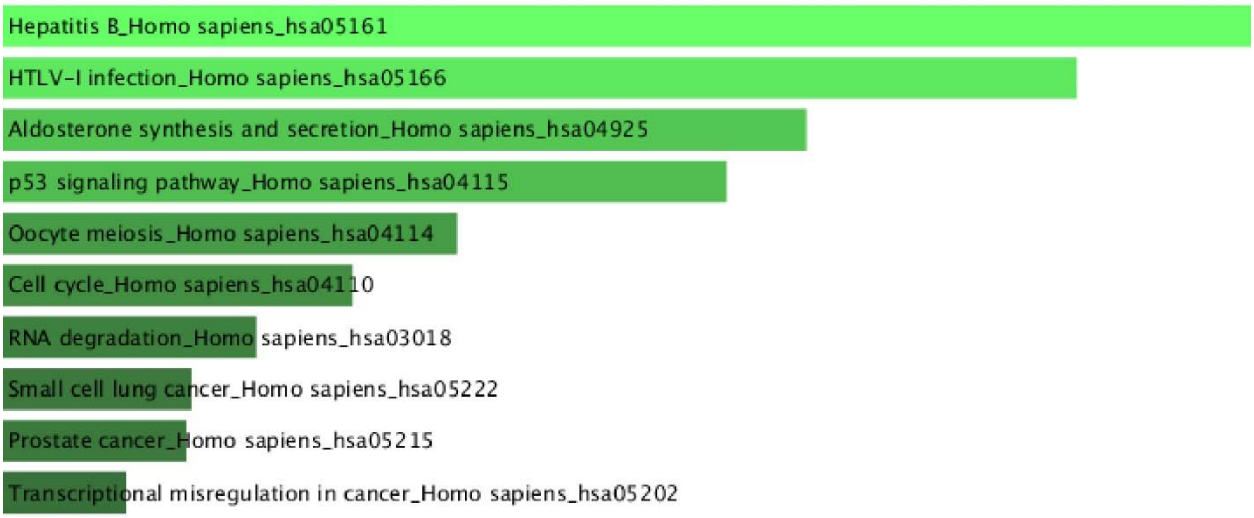


**Figure S11. Enrichr analyses: KEGG cell signaling pathways for panels of clustered downregulated genes.**

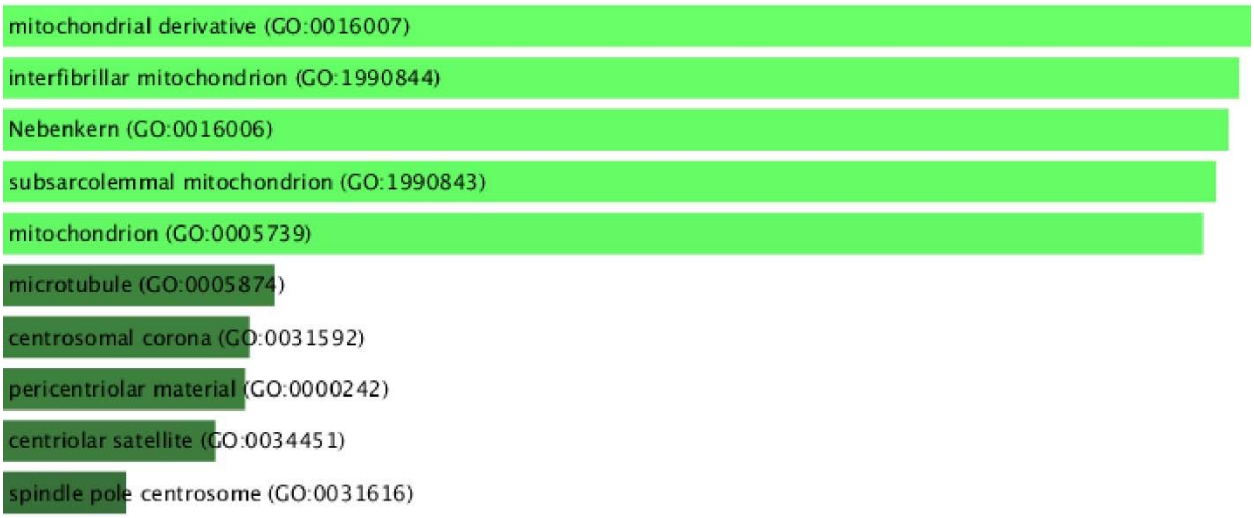


**Figure S12. Enrichr analyses: Cellular components for panels of clustered downregulated genes.**

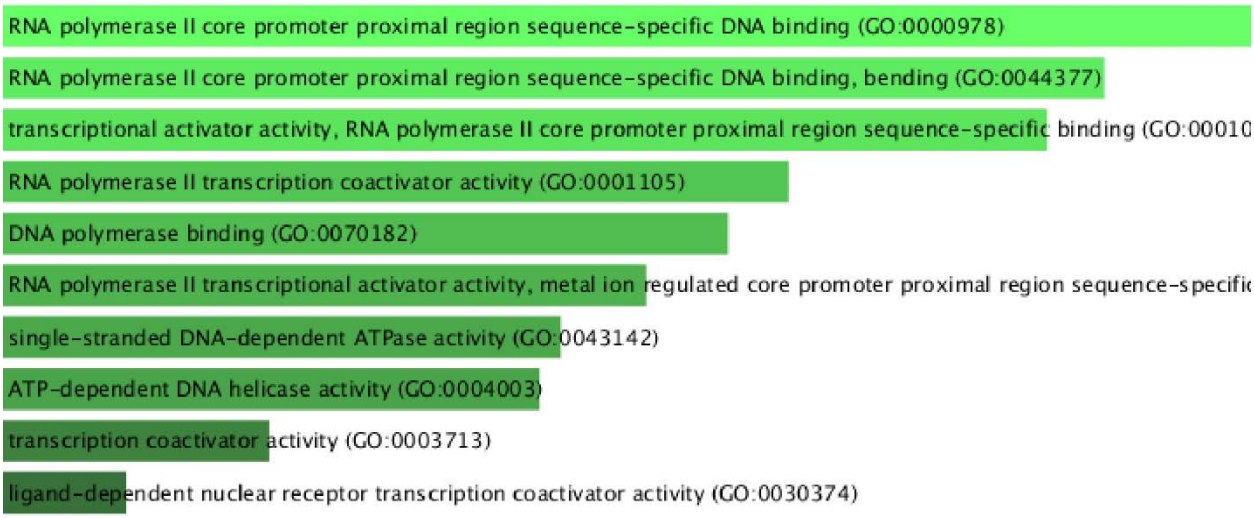


**Figure S13. Enrichr analyses: Molecular function for panels of clustered downregulated genes.**

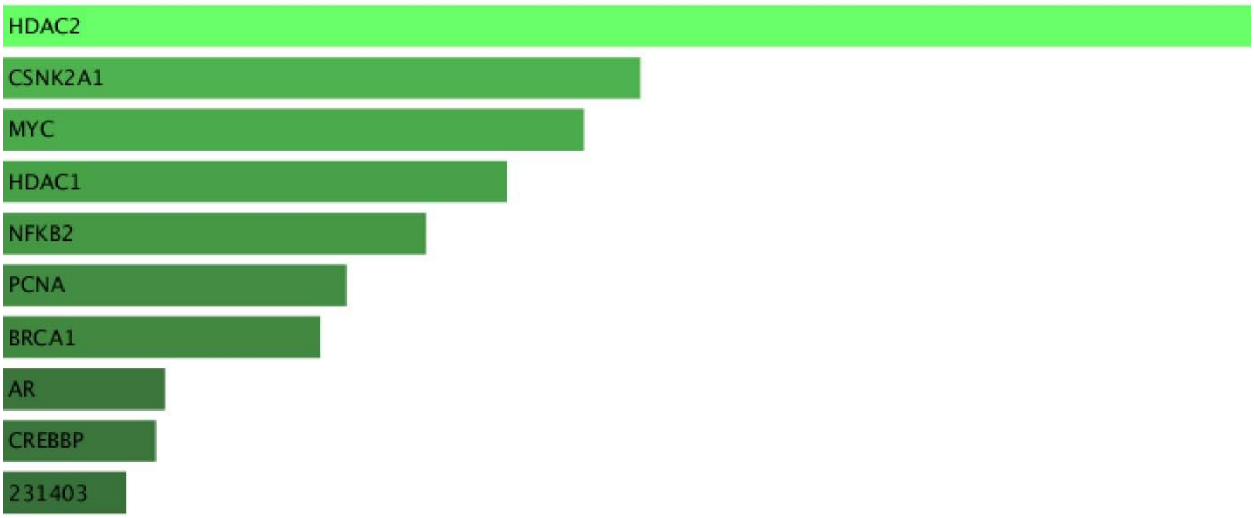


**Figure S14. Enrichr analyses: Protein-protein interaction hubs for panels of clustered downregulated genes.**

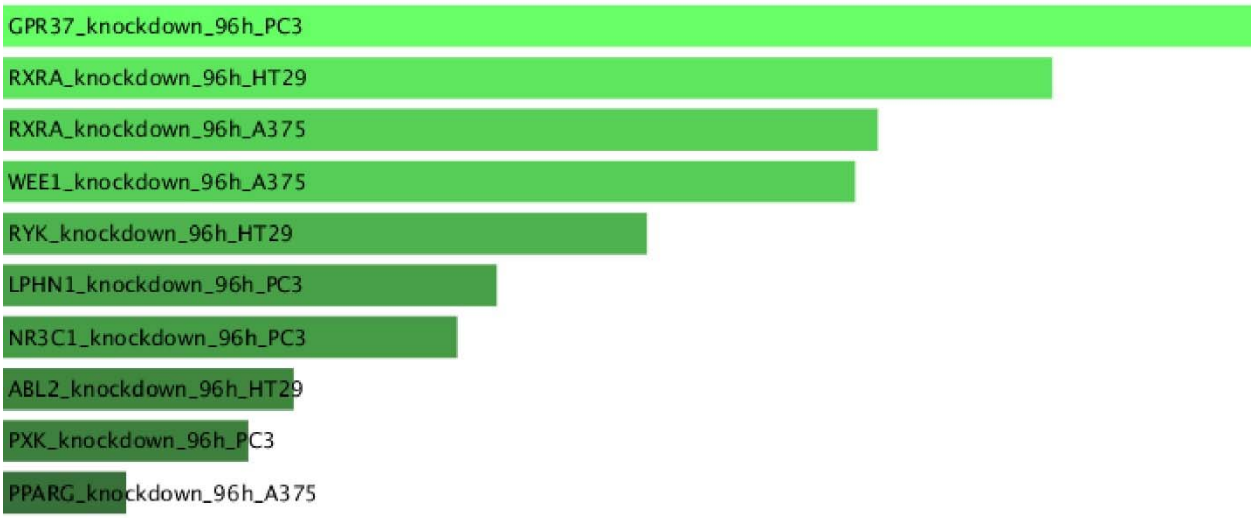


**Figure S15. Enrichr analyses: Kinase analysis for panels of clustered downregulated genes.**

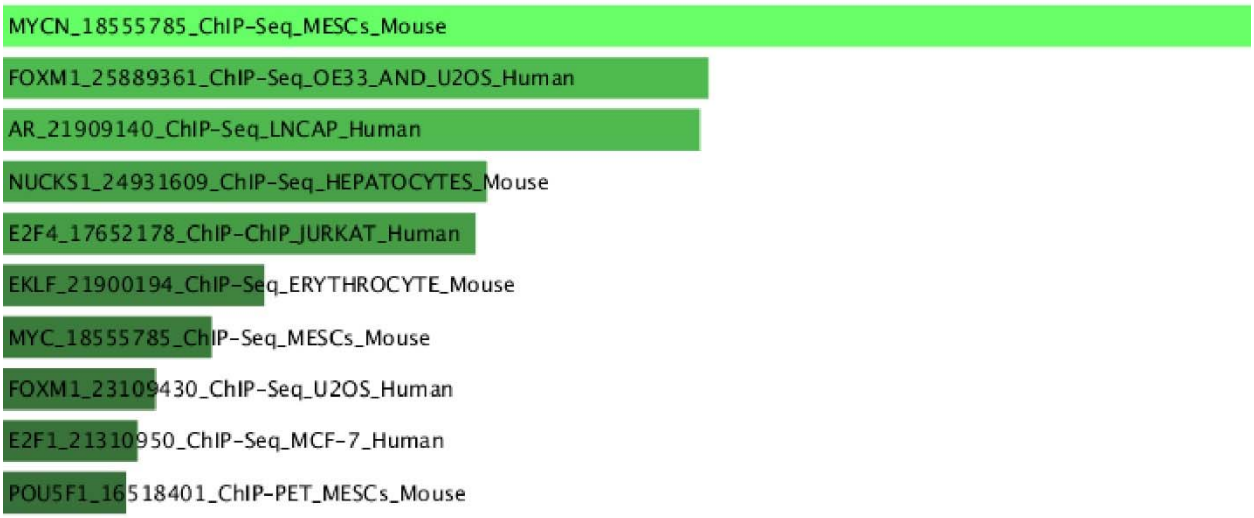


**Figure S16. Enrichr analyses: Transcription factor analysis for panels of clustered downregulated genes.**

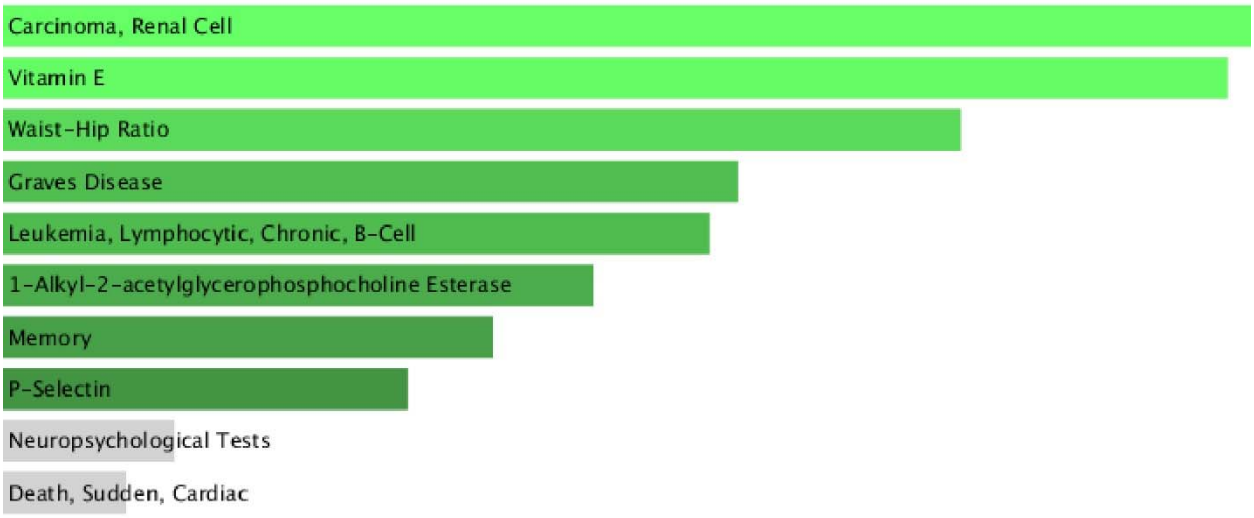


**Figure S17. Enrichr analyses: dbGaP for panels of clustered downregulated genes.**

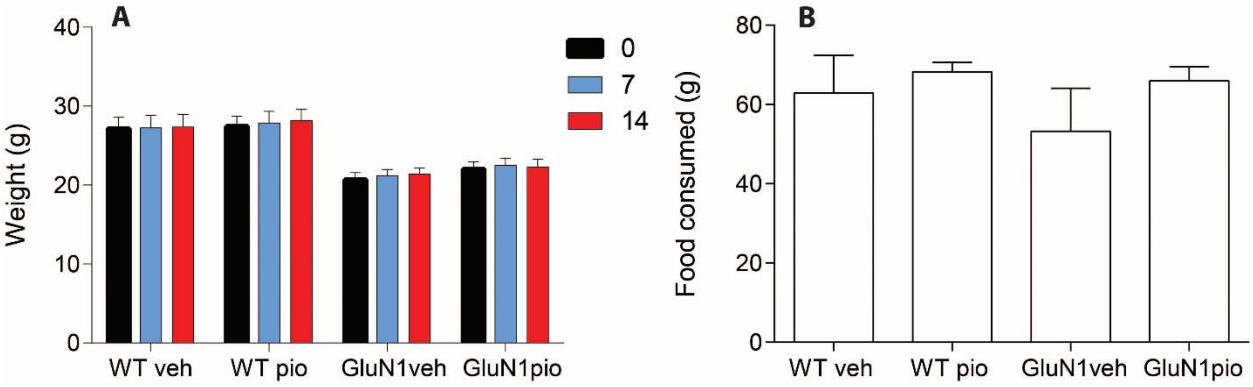


**Figure S18. Animal weight and food consumption.** Average weight (in grams) of groups over 14 days (A). Total amount of food consumed (in grams) by each group over 14 days (B). Data is % mean ± SEM.

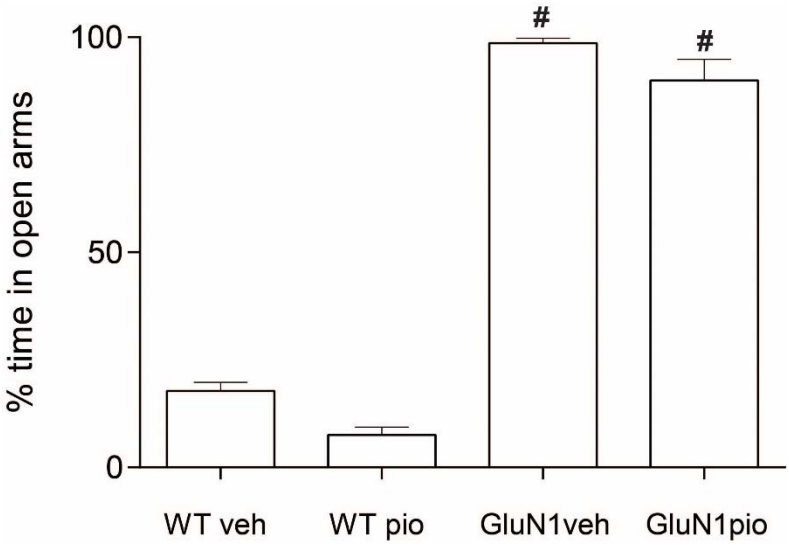


**Figure S19. Elevated plus maze.** Time spent in open arm expressed as % time in open arm versus closed arm. # denotes significantly different from both WTveh and WTpio groups. Data shown as mean ± SEM. $P<0.05$.

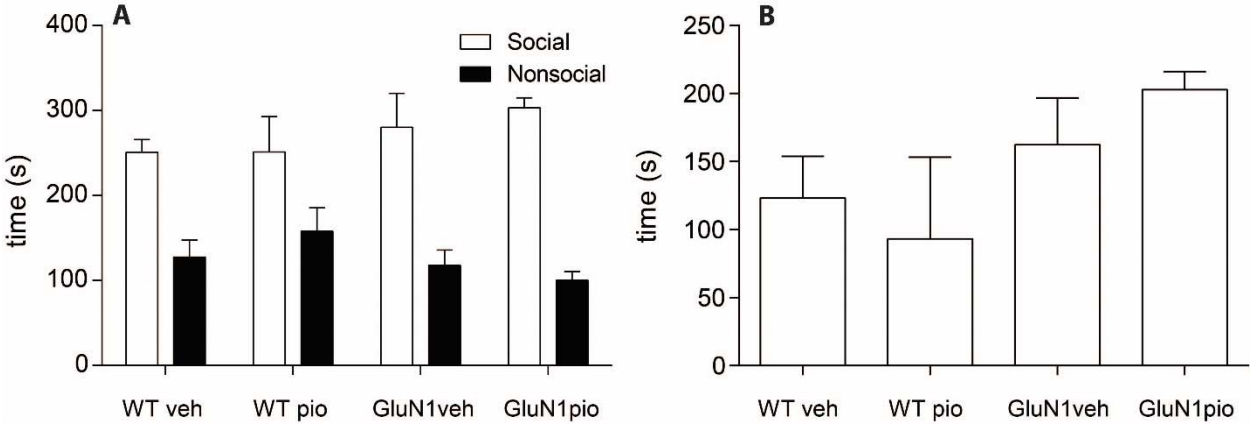


**Figure S20. Social paradigm.** Time (s) spent in social or nonsocial zones distance in the social paradigm for WTveh, WTpio, GluN1veh, and GluN1pio groups (A). Social novelty (time spent in social zone (s) - time spent in nonsocial zone (s)) takes into account that the "cup" that the social mouse is under is also a novel object to the experimental mouse, and takes out the "object novelty" from the data (B). Data shown as mean ± SEM. $P<0.05$.

## SUPPLEMENTARY TABLES

**Summary subjects table.**

| | CTL | SCZ |
|---|---|---|
| N | 16 | 16 |
| Sex | 14m,2f | 14m,2f |
| pH | 6.6±0.2 | 6.6±0.3 |
| PMI | 13±4 | 15±5 |
| Age | 44±9 | 45±11 |
| Rx | 0/16 | 3/11/2 |

**Table S1. Summary demographics of human subjects.**

**Extended subject demographics.**

| # | RIN | Age | PMI | pH | Sex | Suicide | EtOH | Smoking | COD | Medication | Drug abuse? |
|---|---|---|---|---|---|---|---|---|---|---|---|
| Control subjects | | | | | | | | | | | |
| 870 | 5.8 | 28 | 13 | 6.3 | m | no | no | no | electrocution | n/a | n/a |
| 46 | 5.7 | 32 | 10 | n/a | m | no | abuse | n/a | EtOH and narcotic intoxication | n/a | n/a |
| 116 | 4.4 | 49 | 8 | n/a | m | no | n/a | n/a | coronary thrombosis | n/a | n/a |
| 836 | 7.2 | 45 | 18 | 6.97 | m | no | no | no | cardiac arrhythmia | n/a | no |
| 874 | 6.7 | 40 | 7 | 6.67 | m | no | no | yes | cardiac arrhythmia | n/a | n/a |
| 834 | 5.6 | 49 | 19 | 6.67 | m | no | no | no | cardiac arrhythmia | n/a | n/a |
| 80 | 5.5 | 54 | 20 | 6.68 | m | no | n/a | n/a | HASCVD | n/a | n/a |
| 689 | 3.9 | 55 | 10 | 6.87 | m | no | no | no | ASCVD | n/a | no |
| 882 | 7.6 | 37 | 10 | 6.49 | f | no | no | no | DVT | n/a | n/a |
| 828 | 3.9 | 45 | 17 | 6.1 | m | n/a | no | yes | not determined, narcotic intoxication | n/a | no |
| 167 | 3.8 | 41 | 10 | n/a | m | no | n/a | n/a | stab wound, homicide | n/a | n/a |
| 868 | 7.6 | 60 | 15 | 6.98 | m | n/a | n/a | n/a | n/a | n/a | n/a |
| 111 | 4.3 | 23 | 12 | 6.54 | f | n/a | n/a | n/a | n/a | n/a | n/a |
| 859 | 7.4 | 47 | 14 | 6.39 | m | no | no | no | HASCVD | n/a | no |
| 223 | 5 | 44 | 9 | n/a | m | no | n/a | n/a | ASCVD | n/a | n/a |
| 846 | 4.4 | 41 | 6 | 6.6 | m | no | no | n/a | HASCVD | n/a | no |
| Mean ± SD | 5.6 ± 1.3 | 44 ± 9 | 13 ± 4 | 6.6 ± 0.2 | 14m, 2f | | | | | | |

| # | RIN | Age | PMI | pH | Sex | Suicide | EtOH | Smoking | COD | Medication | Drug abuse? |
|---|---|---|---|---|---|---|---|---|---|---|---|
| Schizophrenia subjects | | | | | | | | | | | |
| 29 | 4.7 | 20 | 23 | 6.66 | m | yes | yes | n/a | overdose | Fluphenazine | n/a |
| 94 | 3.5 | 35 | 7 | 6.07 | m | no | abuse | n/a | fatty liver | Fluphenazine | n/a |
| 510 | 7.1 | 34 | 16 | 6.75 | m | yes | n/a | n/a | jumped | Mesoridazine | n/a |
| 737 | 6 | 55 | 12 | 6.35 | m | no | abuse | yes | ASCVD | Atypical | n/a |
| 262 | 7.6 | 42 | 20 | 6.8 | m | n/a | n/a | n/a | inhaled vomit | Typical | n/a |
| 329 | 6.2 | 56 | 25 | 7.1 | m | no | n/a | n/a | ASCVD | Trifluoperazine | n/a |
| 291 | 7.5 | 57 | 9 | 6.43 | m | n/a | dependent | n/a | PE | Thioridazine | n/a |
| 339 | 6.3 | 67 | 8 | 6.36 | m | n/a | dependent | n/a | ASCVD | Typical | n/a |
| 802 | 7.7 | 42 | 14 | 6.8 | f | n/a | probably | n/a | liver cirrhosis | n/a | n/a |
| 446 | 5.4 | 32 | 12 | 6.31 | f | n/a | n/a | n/a | dilated cardiomyopathy | Haloperidol, Mesoridazine | n/a |
| 585 | 6.1 | 42 | 16 | 7.10 | m | no | no | yes | PE | Chlorpromazine, Haloperidol | no |
| 565 | 7.4 | 45 | 16 | 6.66 | m | no | abuse | yes | coronary thrombosis | Chlorpromazine | no |
| 705 | 7.6 | 47 | 16 | 6.47 | m | no | no | yes | DVT | Atypical | no |
| 932 | 6.2 | 54 | 19 | n/a | m | no | abuse | yes | ASCVD | n/a | n/a |
| 331 | 4.8 | 42 | 17 | 6.55 | m | no | abuse | n/a | EtOH intoxication | Thiothixene | no |
| 931 | 4.7 | 42 | 6 | n/a | m | no | abuse | yes | ASCVD | n/a | n/a |
| Mean ± SD | 6.2 ± 1.2 | 45 ± 11 | 15 ± 5 | 6.6 ± 0.3 | 14m, 2f | | | | | | |

**Table S2. Extended demographics of human subjects.**

**Table S3. iLINCS clustering analysis: panels of clustered upregulated and downregulated genes.**

| | Panels of Clustered Upregulated Genes (log2FC) | | | | | |
|---|---|---|---|---|---|---|
| **Gene** | **GPI** | **LDHA** | **PFKM** | **PFKFB2** | **HK1** | **PFKL** |
| MCOLN1 | 0.3772 | 3.877 | 0.1769 | -0.2045 | 0.4864 | 0.5916 |
| GNAI1 | 0.0588 | 2.697 | -0.0615 | 0.5874 | 0.3453 | 0.3772 |
| PIGB | -0.49 | 2.349 | 0.2475 | -0.02386 | -0.2212 | 0.009921 |
| RRP8 | 3.335 | 2.587 | -0.5461 | 1.462 | -0.1273 | -0.5113 |
| MAPKAPK2 | 1.48 | 0.6278 | -0.2539 | -0.3151 | 0.3327 | 0.2047 |
| MAST2 | 1.431 | 0.4499 | 0.0728 | -0.7429 | 0.0133 | 0.3012 |
| LSR | 1.834 | 0.287 | -0.1515 | 0.282 | 0.2576 | 0.401 |
| VAT1 | 1.799 | 0.8464 | 0.3854 | -0.1219 | 0.2661 | 0.1338 |
| CDH3 | 1.109 | -0.5082 | 0.05042 | -0.00234 | 0.1468 | 0.1003 |
| RPS6KA1 | 1.52 | 0.09935 | 0.09849 | 0.1758 | -0.08763 | -0.2001 |
| TWF2 | 1.475 | 0.2866 | 0.2147 | -0.1538 | -0.1449 | -0.1516 |
| RAD9A | 1.379 | 0.1632 | 0.2295 | -0.3141 | -0.2057 | -0.1057 |
| LGMN | 1.395 | 0.1259 | 0.9022 | 0.2079 | -0.1933 | 0.8341 |
| FAM63A | 1.234 | -0.05606 | 1.138 | -0.05397 | -0.1958 | 0.3375 |
| COL1A1 | 1.575 | 0.183 | 0.1555 | -0.1731 | -0.4968 | 0.4655 |
| EFCAB14 | 1.056 | -0.1245 | 0.1694 | -0.1487 | -0.2549 | 0.8911 |
| FOXO4 | 2.496 | 0.134 | 0.8748 | -0.2111 | -0.3544 | 1.347 |
| BAMBI | 1.696 | 0.4097 | 0.8308 | -0.07595 | -0.1352 | 1.29 |
| KDM5B | 1.681 | 0.4324 | -0.1055 | 0.1658 | 1.04 | 1.283 |

| | | | | | | |
|---|---|---|---|---|---|---|
| P4HA2 | 1.603 | 0.2298 | 0.0498 | -0.1318 | 0.8168 | 1.036 |
| PPIC | 1.947 | -0.3411 | 0.3906 | 0.228 | 0.4145 | 0.9223 |
| TSC22D3 | 2.106 | 0.03275 | 0.2558 | -0.1745 | -5.14E-04 | 1.168 |
| ABCC5 | 2.107 | 1.98 | 0.6119 | -0.6195 | 0.3868 | 1.245 |
| RELB | 1.984 | 0.9349 | 0.3671 | -0.6138 | 0.3241 | 0.8325 |
| UBQLN2 | 2.181 | 1.282 | -0.05509 | -0.4613 | -0.12 | 0.8731 |
| FBXO7 | 2.908 | 0.7056 | -0.1333 | -0.2651 | -0.3666 | 0.1958 |
| ARHGEF2 | 2.883 | 0.05977 | 0.004266 | -0.3468 | -0.4032 | 0.04553 |
| MEF2C | 2.662 | 0.754 | -0.1196 | 0.2395 | 0.6507 | 0.06247 |
| SATB1 | 2.837 | 0.1081 | 0.2856 | 0.5636 | 0.6215 | 0.4368 |
| SQRDL | 3.134 | 1.522 | 0.5916 | 0.2194 | -0.06415 | 0.4778 |
| MAPK13 | 4.099 | 0.8354 | 0.335 | -0.3448 | -0.705 | 0.1105 |
| INPP4B | -0.09498 | 1.649 | 0.4987 | 0.388 | 1.266 | 0.5911 |
| CASP2 | -0.2371 | 1.865 | 0.03316 | 0.03125 | 0.3043 | 1.052 |
| SLC35A3 | -0.4248 | 1.057 | 0.8368 | 0.6093 | -0.2008 | 0.09399 |
| C2CD2 | -0.3233 | 0.9543 | -0.09871 | 0.3175 | 0.7076 | -0.1428 |
| GADD45B | -0.2284 | 0.3451 | 0.06478 | 0.1789 | 0.4127 | 1.619 |
| STK10 | -0.566 | 0.2618 | -0.3032 | 0.3348 | 0.4328 | 1.211 |
| FOSL1 | 0.1115 | 0.0639 | -0.4786 | 0.8756 | 0.575 | 1.124 |
| MMP1 | -0.273 | -0.05671 | -0.00879 | 0.297 | 0.2699 | 0.7875 |
| RFNG | 0.09841 | -0.5623 | -0.05895 | 0.4738 | 0.4457 | 0.9216 |
| GADD45A | 0.3943 | -0.141 | -0.3389 | 0.2621 | 0.4765 | 0.9826 |
| BAG3 | 0.5285 | -0.1069 | 0.8774 | -0.2529 | 0.5048 | 0.6179 |
| FBXO11 | 0.3372 | 0.3189 | 0.8422 | -0.5888 | 1.023 | 0.35 |

| | | | | | | |
|---|---|---|---|---|---|---|
| CDKN1A | 0.4662 | -0.5974 | 0.3501 | -0.6747 | 0.2098 | 0.3458 |
| ADRB2 | 0.5395 | -0.1425 | -0.02653 | -0.2553 | 0.8496 | -0.1915 |
| S100A4 | 0.2016 | -0.1601 | 0.2715 | 0.08027 | 0.5794 | 0.261 |
| SSBP2 | 0.2439 | 0.08549 | 0.06745 | -0.3281 | 0.5485 | 0.3621 |
| SMAD3 | 0.5767 | -0.2637 | 0.551 | 0.1963 | 1.048 | 1.287 |
| HYOU1 | 0.7357 | -0.02573 | 0.1409 | -0.213 | 0.6286 | 0.821 |
| CBLB | 1.069 | 0.1808 | 0.1257 | 0.3299 | 0.8466 | 0.7964 |
| ERBB3 | 0.4286 | -0.00342 | 0.9896 | 0.09688 | -0.2027 | 0.8048 |
| UBE2L6 | 0.3547 | -0.1259 | 0.5286 | -0.06399 | 0.00467 | 0.8997 |
| TIPARP | 0.6031 | -0.6833 | 0.4451 | -0.07522 | 0.2736 | 0.8698 |
| FBXL12 | 0.3897 | -0.3633 | 0.7336 | 0.5125 | 0.3267 | 0.6375 |
| IGF2BP2 | 0.2456 | 0.07401 | 1.843 | 0.4604 | 0.213 | 0.4016 |
| ACBD3 | -0.2339 | 0.2138 | 1.103 | -0.04914 | -0.03451 | 0.09469 |
| KIAA0355 | 0.08154 | -0.05733 | 0.706 | 0.2482 | 0.04773 | 0.144 |
| HES1 | 1.026 | 1.43 | 0.6316 | -0.00927 | 0.1819 | 0.8247 |
| FZD7 | 0.5379 | 0.9753 | 1.011 | -0.7442 | -0.02053 | 0.3768 |
| IQGAP1 | 0.3251 | 0.08014 | -0.2069 | -0.06713 | -0.08096 | 0.866 |
| MACF1 | 0.4967 | 0.1458 | -0.1626 | -0.3711 | -0.1319 | 0.9018 |
| MUC1 | -0.1188 | -0.03107 | 0.4661 | -0.177 | -0.3599 | 1.086 |
| SENP6 | 0.08589 | 0.02475 | 0.4488 | -0.2533 | -0.2018 | 0.8971 |
| TMEM2 | 0.01263 | 0.3314 | 0.7077 | -0.1049 | 0.2417 | 1.309 |
| ADAM10 | -0.1032 | 0.5295 | 0.7793 | -0.3765 | -0.05562 | 1.447 |
| HEATR1 | -0.3388 | 0.7431 | 0.362 | -0.1571 | 0.1379 | 0.4458 |
| SCCPDH | -0.09562 | 0.493 | 0.4068 | -0.95 | -0.2563 | 0.8116 |

| | Panels of Clustered Downregulated Genes (log2FC) | | | | | |
|---|---|---|---|---|---|---|
| CNPY3 | -3.271 | -1.134 | -0.3611 | -1.233 | 0.07091 | 0.1877 |
| PPP2R5E | -2.831 | -1.479 | -0.2543 | -0.7931 | 0.2798 | 0.5369 |
| ELOVL6 | -1.333 | 0.1587 | -0.3211 | 1.133 | 0.4316 | -0.8711 |
| MTA1 | -1.247 | 0.2788 | 0.456 | 0.8236 | -0.00311 | -0.2119 |
| SMARCA4 | -0.6969 | 0.2939 | -0.5303 | -0.11 | -0.3327 | -1.489 |
| GTF2A2 | -0.6378 | -0.1805 | 0.03701 | 0.1609 | -0.5999 | -1.271 |
| MYBL2 | -0.6496 | -0.2238 | -0.5386 | 0.09208 | -0.1547 | -0.8986 |
| SLC35F2 | -1.204 | -0.2068 | -0.8753 | -0.1551 | -0.2961 | -0.3806 |
| CCNE2 | -0.617 | 0.08172 | -0.6935 | -0.1196 | -0.2876 | -0.2696 |
| BIRC5 | -1.056 | 0.3306 | -1.227 | 0.09735 | -0.6152 | -0.8805 |
| EXOSC4 | -1.039 | -0.09066 | -1.169 | 0.1816 | -0.1398 | -0.8936 |
| BDH1 | -0.7432 | 0.02569 | -0.9814 | 0.266 | -0.2375 | -0.5965 |
| SCARB1 | -1.074 | 0.002409 | -0.7873 | 0.5655 | -0.3686 | -1.045 |
| MRPL12 | -1.454 | 0.06289 | -0.4946 | 0.4217 | 0.02508 | -1.037 |
| CCDC85B | -1.304 | 0.1394 | -0.7834 | 0.08577 | -0.1551 | -1.039 |
| RUVBL1 | -1.704 | -0.2023 | -0.6445 | 0.3297 | -0.06672 | -0.6351 |
| HADH | -1.468 | -0.3014 | -0.1616 | 0.06154 | -0.3927 | -0.8353 |
| MYCBP | -1.665 | -0.1549 | -0.1827 | 0.01091 | -0.3982 | -0.4436 |
| TXNDC9 | -2.927 | 0.02371 | -1.595 | 0.3875 | -0.3095 | -0.914 |
| HSPD1 | -2.58 | 0.3349 | -0.7643 | 0.1444 | -0.2514 | -0.5682 |
| MYC | -2.914 | 0.01583 | -0.4333 | 0.1788 | -0.2096 | -0.5984 |
| TIMM9 | -2.126 | 0.03366 | -0.3642 | 0.5614 | -0.2764 | -2.116 |
| CHAC1 | -1.906 | 0.2257 | -0.8439 | -0.3551 | 0.05534 | -1.325 |

| | | | | | | |
|---|---|---|---|---|---|---|
| PCBD1 | -1.635 | 0.2792 | -0.2289 | -0.6172 | -0.2265 | -1.116 |
| NFKBIA | -0.01154 | 0.1834 | 0.751 | -1.01 | -0.4948 | -0.06584 |
| SESN1 | 0.0885 | 0.5196 | 0.01913 | -0.6399 | -0.7792 | -0.33 |
| TIMELESS | -0.07703 | 0.04396 | -8.98E-04 | -0.8364 | -0.313 | -0.3432 |
| PRSS23 | -0.8406 | -0.3603 | 0.5509 | -0.1833 | -0.6102 | 0.4304 |
| SLC35A1 | -0.4217 | -0.152 | 1.009 | -0.1151 | -0.8577 | 0.4389 |
| ATF1 | -0.9592 | 0.02308 | 0.619 | 0.1478 | -0.7232 | -0.4905 |
| CLIC4 | -0.6205 | -0.2595 | 0.8741 | -0.4556 | -0.1534 | -0.3473 |
| DLD | -0.7444 | -1.079 | 0.3587 | 0.1603 | -1.006 | -1.535 |
| GNAS | -0.5998 | -0.08384 | 0.4046 | -1.11 | -1.725 | -0.6155 |
| ST7 | -0.1204 | 0.1415 | 0.2135 | -0.834 | -1.9 | -0.9989 |
| TOP2A | 0.1165 | 0.164 | -0.04658 | -0.4499 | -1.476 | -0.9654 |
| LPGAT1 | 0.4376 | -0.06227 | 0.4218 | -0.1752 | -1.325 | -0.8146 |
| HSD17B11 | -0.06855 | -0.3897 | -0.02439 | 0.0648 | -1.561 | -1.036 |
| NT5DC2 | -0.3405 | 0.05698 | -1.03 | -0.5968 | 0.01385 | -0.2579 |
| AURKA | 0.1604 | 0.4304 | -0.5982 | -0.189 | -0.3058 | -0.06925 |
| SLC25A14 | 0.252 | 0.1758 | -0.9508 | -0.3894 | -0.368 | 0.02047 |
| NUSAP1 | -0.2727 | 0.0629 | -0.7033 | -0.6848 | -0.265 | -0.7856 |
| KIF20A | -0.2065 | 0.1954 | -0.4185 | -1.059 | -0.6199 | -0.783 |
| TARBP1 | -0.5917 | -0.1969 | -0.2732 | -0.6185 | -0.9411 | -0.4191 |
| RPIA | -0.9253 | 0.2479 | -0.5214 | -0.6299 | -0.8514 | -0.1086 |
| CREB1 | -0.2295 | -0.5275 | -1.539 | -0.1214 | 0.3761 | 0.2527 |
| ARID4B | 0.0802 | -0.2849 | -1.843 | -0.9948 | 0.007621 | 0.4345 |
| ACD | -0.1577 | -0.7039 | -0.2459 | -0.3494 | 0.2736 | 0.4177 |

| | | | | | | |
|---|---|---|---|---|---|---|
| TESK1 | -0.4087 | -0.5475 | -0.7611 | -0.2312 | 0.2593 | 0.58 |
| CEP57 | 0.6095 | -0.7896 | -0.4846 | -0.4086 | -0.03466 | 0.5022 |
| TCEA2 | 0.4269 | -0.5705 | -0.7747 | -0.0271 | 0.2518 | 0.281 |
| HERPUD1 | -0.5724 | -0.457 | 0.727 | -0.8871 | -0.2887 | 0.4465 |
| IGFBP3 | -1.247 | 0.02535 | 0.4743 | -1.141 | -0.3965 | 0.6744 |
| ABCF1 | -0.06232 | -0.148 | 0.1877 | -1.992 | -0.3513 | 0.44 |
| NISCH | -0.1382 | -0.5247 | 0.0427 | -1.352 | -0.1844 | -0.1797 |
| ZNF318 | 0.04082 | -0.1978 | -0.02954 | -0.7561 | -0.03919 | 0.3409 |
| H2AFV | -0.1653 | -0.02101 | -0.1813 | -1.087 | 0.06698 | 0.2198 |
| CCDC86 | -0.4383 | -0.7162 | -0.3966 | -1.401 | 0.8765 | 0.5771 |
| PSMD2 | -0.8513 | -0.8248 | 0.1684 | -2.7 | 0.4141 | 0.03662 |
| HOXA10 | 0.5374 | 0.5133 | -0.493 | -2.394 | -0.3008 | -1.073 |
| PCNA | 0.816 | -0.03312 | -0.1007 | -3.244 | -1.373 | -1.402 |
| ENOPH1 | -1.559 | 0.3324 | 0.1361 | -3.533 | -0.327 | -2.099 |
| TM9SF3 | -0.4354 | 0.1684 | 0.5067 | -3.233 | -0.4666 | -1.892 |
| IKBKAP | -1.857 | -0.7617 | -0.1593 | -1.786 | -1.052 | -1.163 |
| RFC5 | -1.385 | -0.02085 | -0.7831 | -2.119 | -0.1152 | -0.9693 |
| PFKL | 0.3377 | 0.2806 | -0.7247 | -0.2471 | -0.16 | -3.977 |
| MRPS2 | -1.123 | 1.181 | -1.213 | -1.356 | -0.03834 | -1.459 |
| STUB1 | -0.4753 | 0.4507 | -2.851 | -0.09071 | -0.4586 | -1.645 |
| GNPDA1 | -0.164 | 0.06556 | -1.666 | 0.6103 | -1.14 | -0.6724 |
| CCNB2 | -0.2014 | 0.2726 | -1.734 | -0.1822 | -0.8834 | -0.8978 |

**Table S3. iLINCS clustering analysis: panels of clustered upregulated and downregulated genes.** Log 2 fold change (FC) values are presented for each upregulated and downregulated L1000 gene for each seed gene knockdown (KD) signature.

**Table S4. Top 20 discordant chemical perturbagen signatures per seed gene.**

| Perturbagen | Seed Gene | Concordance | Cell Line |
|---|---|---|---|
| Trifluoperazine | HK1 | -0.415168 | VCAP |
| Tretinoin | HK1 | -0.397106 | VCAP |
| Valproic acid | HK1 | -0.394195 | VCAP |
| ST013886 | HK1 | -0.393411 | VCAP |
| MLS002473819 | HK1 | -0.385526 | VCAP |
| Dexlansoprazole | HK1 | -0.382007 | VCAP |
| ZINC01041848 | HK1 | -0.378767 | VCAP |
| AC1NSIF7 | HK1 | -0.377518 | VCAP |
| Troglitazone | HK1 | -0.377088 | VCAP |
| CHEMBL1884008 | HK1 | -0.37223 | VCAP |
| Flumazenil | HK1 | -0.371409 | VCAP |
| C23H24O8 | HK1 | -0.370781 | VCAP |
| AS-605240 | HK1 | -0.36999 | VCAP |
| Icillin | HK1 | -0.369856 | VCAP |
| Flupirtine | HK1 | -0.366641 | VCAP |
| MLS000106215 | HK1 | -0.362383 | SNUC5 |
| MEGXP0_001444 | HK1 | -0.3611 | VCAP |
| Tretinoin | HK1 | -0.359876 | VCAP |
| N-(3-acetamidophenyl)-3-chlorobenzamide | HK1 | -0.358692 | HCC515 |
| NS-3694 | HK1 | -0.357018 | VCAP |
| BRD-K31310964 | LDHA | -0.297294 | VCAP |

| | | | |
|---|---|---|---|
| BRD-K27503016 | LDHA | -0.282251 | VCAP |
| CGP-37157 | LDHA | -0.281405 | VCAP |
| Parachlorophenol | LDHA | -0.281004 | VCAP |
| BRD-K45231869 | LDHA | -0.27851 | VCAP |
| PF 3845 | LDHA | -0.277911 | HCT116 |
| UK 356618 | LDHA | -0.276899 | A549 |
| AGK 2 | LDHA | -0.275713 | HCT116 |
| BRD-K75393430 | LDHA | -0.272569 | VCAP |
| BRD-K04627808 | LDHA | -0.271066 | VCAP |
| BRD-K19914944 | LDHA | -0.270857 | VCAP |
| MLS003130344 | LDHA | -0.269348 | VCAP |
| PP-30 | LDHA | -0.268455 | HCT116 |
| COT-10B | LDHA | -0.265997 | HEPG2 |
| BRD-K12342216 | LDHA | -0.265288 | VCAP |
| Tangeretin | LDHA | -0.264339 | VCAP |
| HY-11007 | LDHA | -0.264185 | BT20 |
| BRD-K15761174 | LDHA | -0.263793 | VCAP |
| BRD-K68657207 | LDHA | -0.263426 | VCAP |
| CHEMBL586058 | LDHA | -0.262891 | HA1E |
| BRD-K59159285 | GPI | -0.241463 | VCAP |
| Zileuton | GPI | -0.218711 | HCT116 |
| teicoplanin | GPI | -0.209458 | HA1E |
| Fenobam | GPI | -0.208505 | ASC |

| | | | |
|---|---|---|---|
| CHEMBL164433 | GPI | -0.20846 | BT20 |
| Minoxidil | GPI | -0.206587 | A549 |
| M3M3FBS | GPI | -0.203581 | AGS |
| Rimexolone | GPI | -0.20113 | ASC |
| Valproic acid | PFKM | -0.285891 | VCAP |
| BRD-K69423345 | PFKM | -0.266742 | VCAP |
| Trifluoperazine | PFKM | -0.206602 | VCAP |
| THZ-2-98-01 | PFKM | -0.204707 | VCAP |
| Valproic acid | PFKL | -0.507504 | VCAP |
| Trifluoperazine | PFKL | -0.479188 | VCAP |
| C23H24O8 | PFKL | -0.442924 | VCAP |
| Thioridazine | PFKL | -0.441215 | VCAP |
| ST013886 | PFKL | -0.440599 | VCAP |
| Tretinoin | PFKL | -0.427624 | VCAP |
| Troglitazone | PFKL | -0.422798 | VCAP |
| Trifluoperazine | PFKL | -0.422663 | VCAP |
| Fluphenazine | PFKL | -0.418354 | VCAP |
| Tretinoin | PFKL | -0.41519 | VCAP |
| MLS001214919 | PFKL | -0.413819 | VCAP |
| Thioridazine | PFKL | -0.410137 | VCAP |
| Genistein | PFKL | -0.408439 | VCAP |
| LY-294002 | PFKL | -0.403587 | VCAP |
| Tretinoin | PFKL | -0.392361 | VCAP |

| | | | |
|---|---|---|---|
| MLS000106215 | PFKL | -0.383491 | SNUC5 |
| Fluphenazine | PFKL | -0.383423 | VCAP |
| 423735-93-7 | PFKL | -0.380623 | HCT116 |
| ZINC01041848 | PFKL | -0.371954 | VCAP |
| Troglitazone | PFKL | -0.369054 | VCAP |

**Table S4. Top 20 discordant chemical perturbagens per seed gene.** Up to 20 chemical perturbagens that produce L1000 signatures with the most negative concordance values compared to each seed gene knockdown (KD) signature. Vertebral-cancer of the prostate (VCAP), hexokinase 1 (HK1), lactate dehydrogenase A (LDHA), glucose phosphate isomerase (GPI), phosphofructokinase muscle type (PFKM), phosphofructokinase liver type (PFKL).

**Table S5. Overall top 20 discordant perturbagen signatures.**

| Perturbagen | Seed Gene | Concordance | Cell Line |
|---|---|---|---|
| Valproic acid | PFKL | -0.507504 | VCAP |
| Trifluoperazine | PFKL | -0.479188 | VCAP |
| C23H24O8 | PFKL | -0.442924 | VCAP |
| Thioridazine | PFKL | -0.441215 | VCAP |
| ST013886 | PFKL | -0.440599 | VCAP |
| Tretinoin | PFKL | -0.427624 | VCAP |
| Troglitazone | PFKL | -0.422798 | VCAP |
| Trifluoperazine | PFKL | -0.422663 | VCAP |
| Fluphenazine | PFKL | -0.418354 | VCAP |
| Tretinoin | PFKL | -0.41519 | VCAP |
| Trifluoperazine | HK1 | -0.415168 | VCAP |
| MLS001214919 | PFKL | -0.413819 | VCAP |
| Thioridazine | PFKL | -0.410137 | VCAP |
| Genistein | PFKL | -0.408439 | VCAP |
| LY-294002 | PFKL | -0.403587 | VCAP |
| Tretinoin | HK1 | -0.397106 | VCAP |
| Valproic acid | HK1 | -0.394195 | VCAP |
| ST013886 | HK1 | -0.393411 | VCAP |
| Tretinoin | PFKL | -0.392361 | VCAP |
| MLS002473819 | HK1 | -0.385526 | VCAP |

**Table S5. Top 20 discordant chemical perturbagens across all seed gene knockdown signatures.** The top 20 chemical perturbagens that produce L1000 signatures with the most negative concordance values compared to any of the seed gene knockdown (KD) signatures. Hexokinase 1 (HK1), phosphofructokinase liver type (PFKL), vertebral-cancer of the prostate (VCAP).

| Mouse ID | GluN1 | Cre | Cage | Age (wks) | Sex | Rx | Dose |
|---|---|---|---|---|---|---|---|
| NLX598.2 | -/- | Tg+ | RAEF | 11.3 | M | PIO | 100ppm |
| NLX599.5 | WT | nTg | RAEF | 11.1 | M | PIO | 100ppm |
| NLX598.3 | -/- | nTg | RAEG | 11.3 | F | PIO | 100ppm |
| NLX599.2 | -/- | Tg+ | RAEG | 11.1 | F | PIO | 100ppm |
| NLX599.1 | WT | Tg+ | RAEH | 11.1 | M | vehicle | 0 |
| NLX599.8 | WT | nTg | RAEH | 11.1 | M | vehicle | 0 |
| NLX600.5 | -/- | Tg+ | RAEI | 10.4 | M | vehicle | 0 |
| NLX600.7 | WT | Tg+ | RAEI | 10.4 | M | vehicle | 0 |
| NLX642.2 | -/- | Tg+ | RAGH | 12.3 | F | PIO | 100ppm |
| NLX642.9 | -/- | nTg | RAGH | 12.3 | F | PIO | 100ppm |
| NLX643.1 | -/- | nTg | RAGH | 12.3 | F | PIO | 100ppm |
| NLX643.6 | WT | Tg+ | RAGH | 12.3 | F | PIO | 100ppm |
| NLX644.1 | -/- | nTg | RAGN | 10.7 | F | vehicle | 0 |
| NLX645.2 | -/- | nTg | RAGN | 10.7 | F | vehicle | 0 |
| NLX645.6 | WT | Tg+ | RAGN | 10.7 | F | vehicle | 0 |
| NLX645.7 | WT | Tg+ | RAGN | 10.7 | F | vehicle | 0 |
| NLX644.5 | WT | nTg | RAGM | 10.7 | M | PIO | 100ppm |
| NLX644.9 | -/- | nTg | RAGM | 10.7 | M | PIO | 100ppm |
| NLX645.4 | WT | nTg | RAGM | 10.7 | M | PIO | 100ppm |
| NLX644.2 | -/- | nTg | RAGL.1 | 10.7 | F | vehicle | 0 |
| NLX644.4 | -/- | nTg | RAGL.1 | 10.7 | F | vehicle | 0 |
| NLX644.7 | WT | nTg | RAGL.2 | 10.7 | F | PIO | 100ppm |
| NLX644.8 | -/- | nTg | RAGL.2 | 10.7 | F | PIO | 100ppm |
| NLX647.6 | WT | Tg+ | RAGP.1 | 10.1 | M | vehicle | 0 |
| NLX647.7 | WT | nTg | RAGP.1 | 10.1 | M | vehicle | 0 |
| NLX647.9 | WT | nTg | RAGP.2 | 10.1 | M | PIO | 100ppm |
| NLX646.2 | WT | nTg | RAGP.2 | 10.0 | M | PIO | 100ppm |
| # NXD31.6 | -/- | nTg | RAJB | 13.6 | M | PIO | 100ppm |

| | | | | | | | |
|---|---|---|---|---|---|---|---|
| # NXD33.3 | -/- | nTg | PIO | 10.9 | F | PIO | 100ppm |
| # NLX709.2 | -/- | Tg+ | PIO | 11.9 | F | PIO | 100ppm |
| # NLX708.1 | -/- | Tg+ | RAJE | 11.9 | M | vehicle | 0 |
| # NLX708.6 | WT | Tg+ | RAJE | 11.9 | M | vehicle | 0 |
| # NLX710.4 | WT | Tg+ | RAJI | 11.4 | M | PIO | 100ppm |
| # NLX710.6 | WT | nTg | RAJI | 11.4 | M | PIO | 100ppm |
| # NLX720.1 | -/- | nTg | RAJR | 8.9 | F | vehicle | 0 |
| # NLX720.3 | WT | nTg | RAJR | 8.9 | F | vehicle | 0 |
| # NLX721.1 | WT | Tg+ | RAJS | 8.7 | M | vehicle | 0 |
| # NLX721.3 | WT | Tg+ | RAJS | 8.7 | M | vehicle | 0 |
| # WAV271.1L | WT | Tg+ | RAJS | 8.1 | M | vehicle | 0 |
| # NLX722.5 | -/- | nTg | RAJU | 8.6 | F | PIO | 100ppm |
| # NLX723.6 | WT | Tg+ | RAJU | 8.1 | F | PIO | 100ppm |
| # NLX723.2 | -/- | nTg | RAJT | 8.1 | M | vehicle | 0 |
| # NLX723.4 | -/- | Tg+ | RAJT | 8.1 | M | vehicle | 0 |

**Table S6. Demographics on GluN1 KD mice from pioglitazone study.** Demographics on GluN1 KD and wildtype mice used in pioglitazone studies. # denotes additional mice used in locomotor task and puzzle box assay.

**Experimental timeline for behavioral assays.**

| Behavioral Assay | Endophenotype | Day of experiment |
|---|---|---|
| Open Field Test | Hyperactivity and Stereotypy | 7 |
| Elevated Plus Maze | Anxiety | 9 |
| Puzzle Box Assay | Executive Function | 10-12 |
| Social Paradigm | Social Behaviors | 15 |
| Prepulse Inhibition | Sensorimotor Gating | 16 |

**Table S7. Behavioral assay timeline.** On days 1-6, mice began a diet of either vehicle or pioglitazone chow. On Day 7, all mice had their locomotor activity and stereotypy behavior measured in the Open Field Test. On day 9, mice were tested on the Elevated Plus Maze (EPM). Days 10 through 12, mice were tested in the puzzle box assay. Day 15 mice were subjected to the social affiliative paradigm, and finally on day 16, pre-pulse inhibition was tested.